Proceedings of ISAP'04, Sendai, JAPAN

# PATH LOSS MEASUREMENTS OF ON-BODY PROPAGATION CHANNELS

Yuriy NECHAYEV[1], Peter HALL[1], Costas CONSTANTINOU[1], Yang HAO[2], Abdus OWADALLY[2], and Clive PARINI[2]
[1]Department of Electronic, Electrical and Computer Engineering, the University of Birmingham
Edgbaston, Birmingham B15 2TT, UK
[2]Department of Electronic Engineering, Queen Mary, University of London
Mile End Road, London E1 4NS, UK
E-Mail P.S.Hall@bham.ac.uk

## 1. Introduction

Ever growing miniaturisation of electronic devices combined with the recent developments in wearable computer technology have been leading to creation of a wide range of devices which can be carried by their user in the pocket or attached to their body in any other way [1]. Using wired connections between such devices is often undesirable because of their inconvenience for a user. A number of other connection methods have been proposed for this purpose, including smart textiles and communication by the currents in the user's body. Each of these methods has their own advantages and drawbacks. Among the drawbacks of the smart clothes, for example, we can mention a need for a special garment to be worn, which may conflict with the user's personal preferences.

Wireless radio connectivity is another obvious option for connecting body worn devices. Several standards for wireless connections between such devices have been developed, including Bluetooth, BodyLAN and Zigbee. This type of connection can provide great level of flexibility and comfort to the user and therefore has received a lot of attention. Efficient design of devices using wireless connections requires good understanding of the properties of the propagation channel involved. Therefore, a number of path loss measurements of several types of on-body propagation channels have been undertaken. The results will be presented in this paper together with the estimates of other important propagation channel parameters, such as delay spread and coherence bandwidth.

## 2. Measurement Setup

Propagation path loss of an on-body channel was measured using a vector network analyser (VNA). Two 8.6 dBi patch antennas were positioned on the body at a number of positions and orientations and connected to the calibrated VNA by two 5 m long flexible coaxial cables. For each antenna placement setup, $S_{21}$ response was then measured every second while the person wearing the antennas assumed various body positions changing them every 20 s. The positions of the antennas on the body are shown in Fig. 1 and the body positions used in all the measurements are listed in Table I. Each measurement set was repeated twice: once inside an anechoic chamber and once outside, in the laboratory.

## 3. Results and Discussion

On-body propagation links can be roughly categorised according to the parts of the body to which the transmit and receive antennas are attached, e.g. trunk-to-trunk, trunk-to-head, trunk-to-hand etc. Characteristics of the propagation channels corresponding to different types of such links can be expected to differ considerably due to highly varying variability of the link. Thus, for example, a trunk-to-limb link is expected to be subject to significant variation due to the movement of the limb while a trunk-to-trunk link will be more stable.

Fig. 2 presents some of the measurement results for scenarios when both antennas are on the trunk of the body. In all the presented measurements the transmit antenna was placed on the belt on the left front side of the body (position Tx in Fig. 1) and polarised either vertically or horizontally. The results for the vertically oriented receiver on the right side of the chest (position Rx1 in Fig. 1) and the transmitter vertically and horizontally oriented are shown as the solid and dashed line, respectively, in

ISBN: 4-88552-207-2 C3055©IEICE

Fig. 3. The dotted line corresponds to the receiver on the left side of the upper back (Rx2 in Fig. 1) and both antennas vertically oriented. In the rest of the measurements, the transmitter was always vertically oriented on the belt at position Tx.

Trunk-to-head and trunk-to-hand scenarios are represented in Figs. 2 and 3, respectively. In these figures, the solid lines correspond to the vertically oriented receiver on the left side of the head (Fig. 3) or on the left wrist (Fig. 4), and the dashed lines, to the vertically oriented receiver on the right side of the head or wrist. The dotted line in Fig. 4 represents the case when the receive antenna is horizontally oriented on the left wrist. These receiver positions are depicted in Fig. 1 as positions Rx3–Rx6. All path gain values in the plots are limited at the lower end by –70 dB level corresponding to the noise floor.

Comparing the results taken in the anechoic chamber and in the laboratory shows a noticeable increase in signal variability outside the anechoic chamber due to multipath fading. Outside the chamber, the propagation channel is not stable even when the body is still. This is caused by people moving in the room. As can be seen from the in-chamber measurements, variations due to breathing and/or other small body movements are no more than about 4 dB, which agrees with the results reported in [2]. Spread of values due to changing body positions, on the other hand, reaches a maximum of 26, 36 and 44 dB, respectively, for the trunk-to-trunk, trunk-to-head and trunk-to-hand measurements in the anechoic chamber. The corresponding values for the measurements outside the chamber are 30, 37 and 40 dB, respectively. The minimum and maximum values for the channel path gain (PG) are summarised in Table II.

The results show that the major source of variability in the channel is movement of the parts of the body to which the antennas are attached relative to each other. These movements cause variations of the distance between the antennas as well as possible shadowing and polarisation detuning. The variability is especially severe when one of the antennas is positioned on a hand, which is highly mobile. Variations are further increase outside the anechoic chamber by multipath fading. In most of the measurements, the average signal level is also higher outside the chamber than inside due to increased amount of scattered power reaching the receiver.

Although the time delays of on-body propagation paths were not measured, they can be estimated from the dimensions of the body. Path lengths on the body cannot exceed approximately 1–2 m, depending on the antenna positions, which leads to a maximum time delay of 3–7 ns. However, it is evident from the measured path gains that the environment around the body can significantly contribute towards the received signal. Therefore, the paths scattered from the surrounding objects will increase the delay spread. Inside a room, the singly scattered path lengths are of the order of twice the room dimension. For, say, a 5 m long room this gives a rough estimate for the time delay of $\tau = 33$ ns corresponding to the coherence bandwidth $B_c \cong 1/\tau = 30$ MHz. For a more accurate prediction direct measurements of the time delay are required.

## 4. Conclusions

A set of path loss measurements of on-body propagation channels at 2.4 GHz inside and outside an anechoic chamber has been presented. The channel was shown to exhibit high variability caused by relative movements of the body parts with the antennas on them. Therefore, a large number of measurements of an on-body propagation channel is needed for appropriate characterisation of the channel. Measurements of the time delay are also required although a very large bandwidth (300 MHz and above) is necessary to resolve different propagation paths on the body.

## 5. Acknowledgements

This work has been supported by an EPSRC grant and by the Ministry of Defence (UK).

## 6. References

[1] S. I. Woolley, J. W. Cross, S. Ro, R. Foster, G. Reynolds, C. Baber, H. Bristow, and A. Schwirtz, "Forms of wearable computer," presented at IEE Eurowearable'03, Birmingham, UK, 2003.

[2] P. S. Hall, M. Ricci, and T. W. Hee, "Characterization of on-body communication channels," presented at the 3rd ICMMT, 2002.

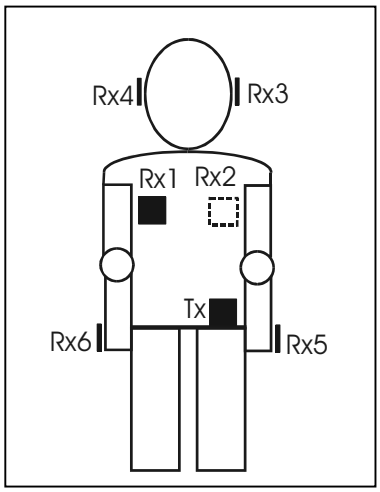


Figure 1. Antennas on a body

Table I. Body Positions

| N | Time Slot (s) | Body Position |
|---|---|---|
| 1 | 0 – 20 | Standing upright still |
| 2 | 20 – 40 | Standing, body turned to the left |
| 3 | 40 – 60 | Standing, body turned to the right |
| 4 | 60 – 80 | Standing, body slightly leaned forward |
| 5 | 80 – 100 | Standing upright, head leaned forward |
| 6 | 100 – 120 | Standing upright, head turned to the left |
| 7 | 120 – 140 | Standing upright, head turned to the right |
| 8 | 140 – 160 | Standing upright, arms stretched out to the sides |
| 9 | 160 – 180 | Standing upright, arms above the head |
| 10 | 180 – 200 | Standing upright, arms reaching forward |
| 11 | 200 – 220 | Standing upright, lower arms reaching forward |
| 12 | 220 – 240 | Moving arms, head and body freely while standing |
| 13 | 240 – 260 | Sitting still on a stool, arms hanging along the body |
| 14 | 260 – 280 | Sitting still on a stool, hands in the lap |
| 15 | 280 – 300 | Moving arms, head and body freely while sitting |
| 16 | 300 – 320 | Standing upright still |
| 17 | 320 – 340 | Walking back and forth, arms close to the body |
| 18 | 340 – 360 | Moving arms, head and body freely while walking back and forth |

Table II. Variability of On-Body Propagation Channels

| | Measurement | Inside anechoic chamber | | Outside anechoic chamber | |
|---|---|---|---|---|---|
| | | Min. PG (dB) | Max. PG (dB) | Min. PG (dB) | Max. PG (dB) |
| Trunk-to-Trunk | Rx on chest, co-pol. | -48 | -34 | -56 | -32 |
| | Rx on chest, cross-pol. | -64 | -38 | -69 | -39 |
| | Rx on back | -70 | -50 | -70 | -45 |
| Trunk-to-Head | Rx on the left side of head | -70 | -34 | -55 | -26 |
| | Rx on the right side of head | -70 | -37 | -60 | -22 |
| Trunk-to-Hand | Rx on left wrist, co-pol. | -69 | -24 | -70 | -33 |
| | Rx on right wrist, co-pol. | -70 | -41 | -70 | -44 |
| | Rx on left wrist, cross-pol. | -70 | -28 | -67 | -27 |

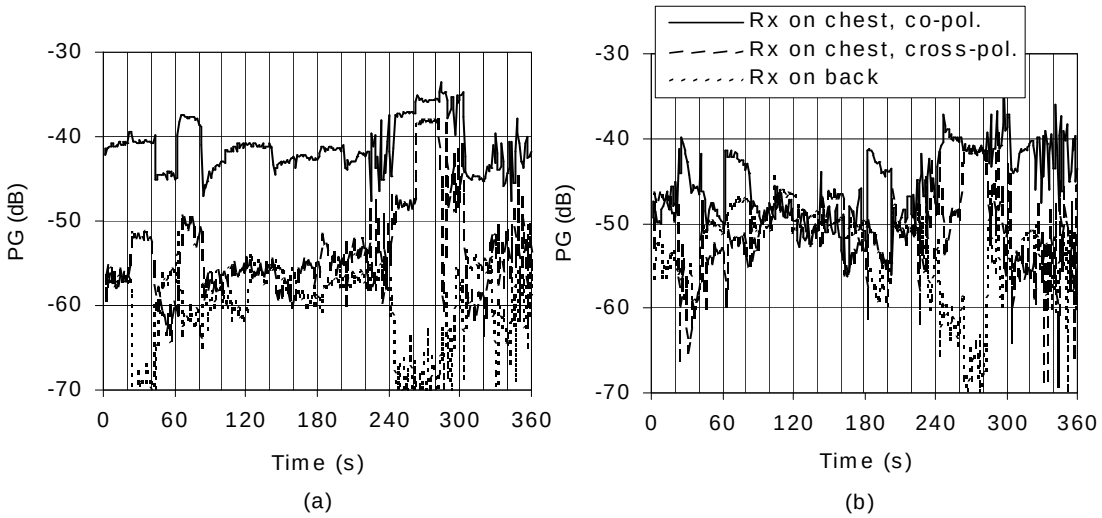


Figure 2. Trunk-to-trunk measurements (a) in the anechoic chamber, (b) in the lab

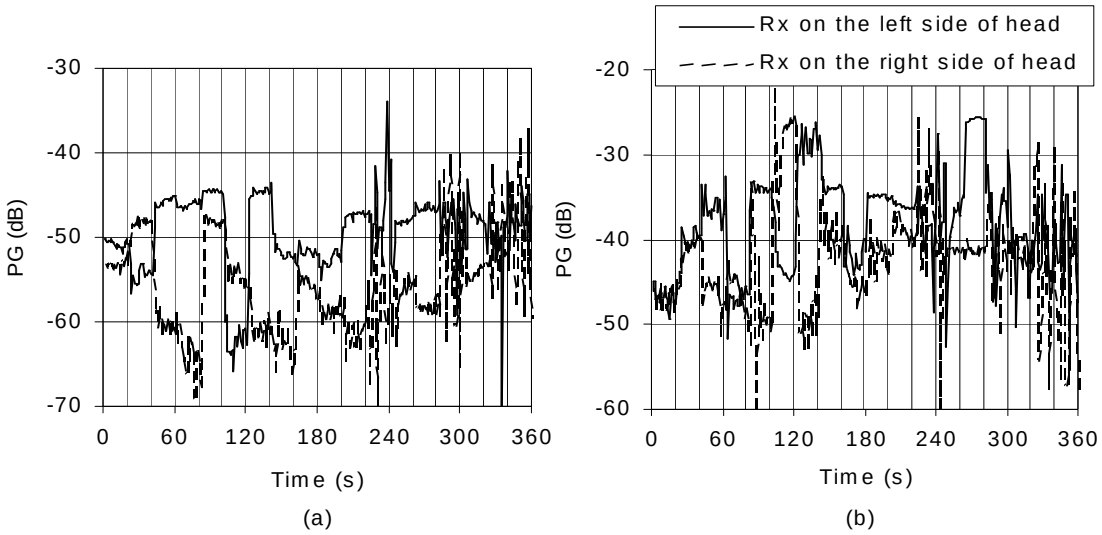


Figure 3. Trunk-to-head measurements (a) in the anechoic chamber, (b) in the lab

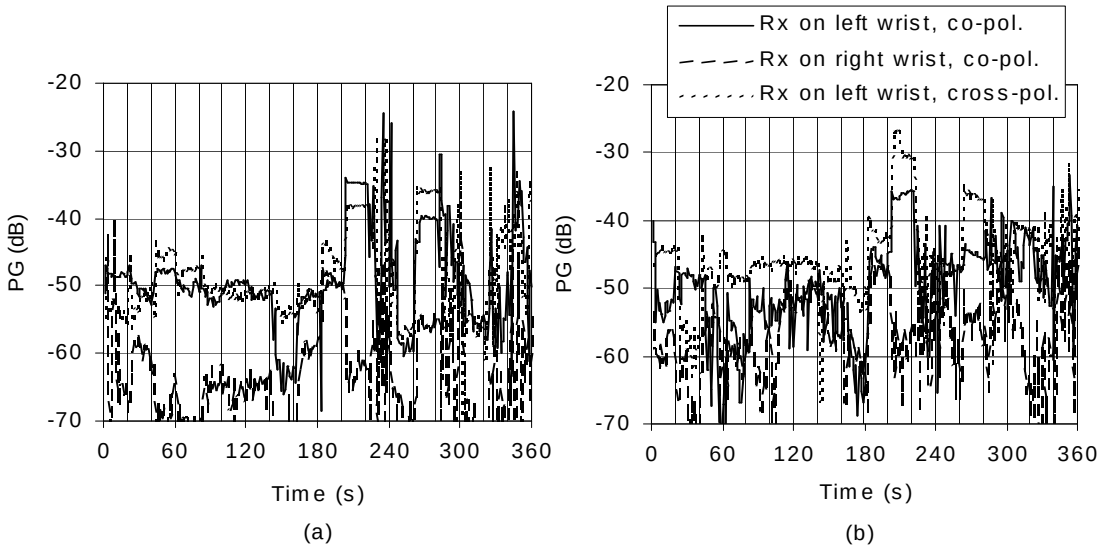


Figure 4. Trunk-to-hand measurements (a) in the anechoic chamber, (b) in the lab